AIP Conference Proceedings

Seismodynamics of an extended underground pipeline based on a nonlinear model of interaction with the ground

Cite as: AIP Conference Proceedings **2637**, 030004 (2022); https://doi.org/10.1063/5.0118457
Published Online: 20 October 2022

Ibrakhim Mirzaev and Jakhongir F. Shomurodov

Seismodynamics of an Extended Underground Pipeline Based on a Nonlinear Model of Interaction with the Ground

Ibrakhim Mirzaev [1, a)] and Jakhongir F. Shomurodov [2, b)]

[1]*Institute of Mechanics and Seismic Stability of Structures named after M.T. Urazbaev, Durmon yuli Str. 33, Tashkent 100125, Uzbekistan.*
[2]*Tashkent State Transport University, Odilxojayev Str. 1, Tashkent, Uzbekistan.*

[a)]*Corresponding author: ibrakhim.mir@mail.ru*
[b)]*jakhongir_shf@mail.ru*

Abstract. The piecewise linear problem of the effect of a seismic wave propagating in the ground on an extended underground pipeline interacting with the ground has been solved by the explicit finite difference method according to a model, that takes into account the process of destruction of the soil structure. This model reflects experimental data on soils. The nonlinear interaction model is approximated by a piecewise linear model. The problems of the effect of a high-frequency harmonic wave propagating in the ground on an underground pipeline in the case of nonlinear interaction were previously solved by the method of characteristics. An explicit finite-difference scheme is constructed an iterative process is used to refine the solution during the transition from one state to another state of the coefficient of interaction of the pipeline with the ground. The results of calculating velocities, deformations, displacements and lateral tangential stresses for different waveforms are presented. A comparison is made with the solutions of the problems of elastic interaction and interaction according to an ideally elastic-plastic model.

Keywords: elasticity, plasticity, fracture, friction, wave, pipe, soil.

INTRODUCTION

The study of the behavior of underground pipelines as a life support system during earthquakes is an important task. An overview of the work in this direction has given in [1-3, 14-16]. Some underground utilities are built and operated in earthquake-prone areas [13-19]. This circumstance requires reliable seismic safety of underground structures and pipelines [15-17]. Experimental studies [1, 2, 4] allowed us to substantiate simplified models of viscoelastic and elastoplastic interaction of soil and pipeline. Here, under certain conditions, the main role is played by the soil property, this is confirmed by the experiments carried out to determine the shear modulus of fine-grained soil at different loading speeds [5]. In addition, in experimental studies [5, 4] on soils and in the study of the interaction of the pipe with the soil, the destruction of the soil structure was revealed at a sufficient level of shear stress.

In linear problems of seismodynamics of underground structures, the system of equations of motion includes terms without derivatives of displacements and angles of turns [1, 6, 13]. The construction of finite-difference schemes for such equations without parasitic oscillations has given in [7, 8]. Spatial problems for complex systems of underground pipelines are considered in [6, 10].

In nonlinear problems of seismodynamics of underground structures, various models of pipeline-ground interaction are used [12]. The stationary problem of seismodynamics of an extended rectilinear pipeline with nonlinear interaction models using the plasticity function is considered in [11]. The problems of the effect of a harmonic wave

International Conference on Actual Problems of Applied Mechanics - APAM-2021
AIP Conf. Proc. 2637, 030004-1–030004-10; https://doi.org/10.1063/5.0118457
Published by AIP Publishing. 978-0-7354-4229-0/$30.00

propagating in the ground on an underground pipeline in the case of nonlinear interaction were previously solved by the method of characteristics [2, 4].

Non-stationary problems for a rod with external dry friction were solved by the method of characteristics in [20, 21]. A solution for a stationary problem is constructed and the behavior of its solution is described.

In this paper, the problem of seismodynamics of an extended rectilinear underground pipeline with a model of interaction with the destruction of the soil structure is solved by an explicit finite-difference method using a logical algorithm for determining transitions from one state to another state.

MATERIALS AND METHODS

Let a plane longitudinal wave $v_g(t - x/c_g)$ propagate along the ground at a velocity c_g, the normal to the front of which is parallel to the axis of the pipeline of length L. The origin of the coordinate axis *Ox* is located on the left end of the pipeline. Suppose that the movement of the ground is set and is not distorted due to the presence of a pipeline, which is modeled by an elastic rod. At the same time, the interaction of the pipeline with the surrounding soil is taken into account according to a piecewise linear model with the destruction of the soil structure (Fig. 1), the constants of which are determined experimentally, preferably dynamically.

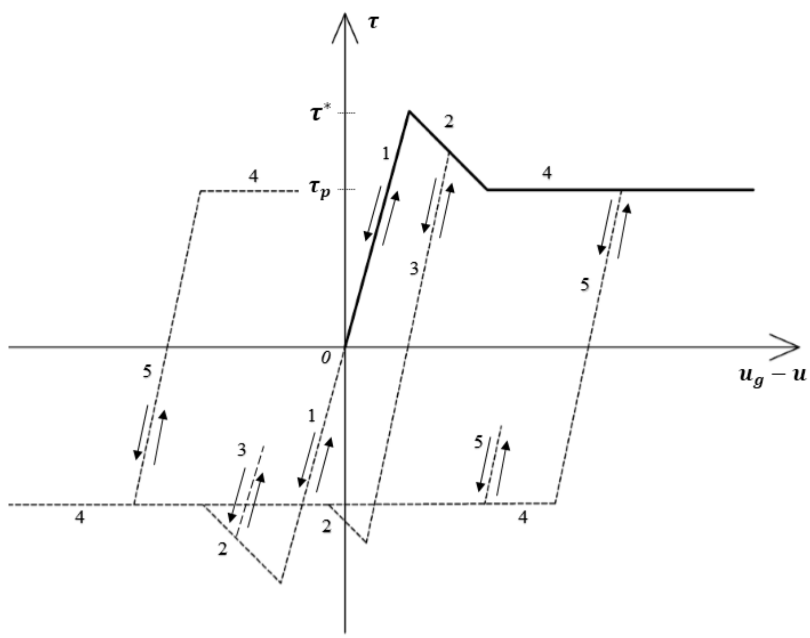

FIGURE 1. Diagram of the $\tau = \tau_s + k_\alpha(x,t)\cdot(u_g - u - U_s)$ dependence corresponding to the piecewise linear law of interaction.

For the mathematical formalization of the piecewise linear interaction model shown in Fig. 1, we introduce a piecewise constant function $S(x,t)$, reflecting information about the state of interaction at point x at time t. The piecewise constant function $S(x,t)$ can take values from 1 to 5.

The equations of dynamics of an extended underground pipeline are presented in the form

$$\begin{aligned} \frac{\partial v}{\partial t} &= c^2 \frac{\partial \varepsilon}{\partial x} + \frac{\pi D}{F\rho}\tau, \\ \frac{\partial \varepsilon}{\partial t} &= \frac{\partial v}{\partial x}, \end{aligned} \qquad (1)$$

$$\tau = k_1(u_g - u), \text{ for } |\tau| \le \tau^* \text{ and } S(x,t)=1;$$
$$\tau = \tau_s + k_2(u_g - u - U_s), \; S(x,t)=2, \text{ for } |\tau| > \tau^* \text{ and } S(x,t)=1;$$
$$\tau = \tau_s + k_2(u_g - u - U_s), \text{ for } S(x,t)=2 \text{ and } |\tau| > \tau_p;$$
$$\tau = \tau_s + k_3(u_g - u - U_s), \; S(x,t)=3, \text{ for } \tau\cdot(v_g - v) < 0 \text{ and } S(x,t)=2;$$
$$\tau = \tau_s + k_3(u_g - u - U_s), \text{ for } S(x,t)=3 \text{ and } |\tau| \le |\tau_s|;$$
$$\tau = \tau_s + k_2(u_g - u - U_s), \; S(x,t)=2, \text{ for } |\tau| > |\tau_s| \text{ and } S(x,t)=3;$$
$$\tau = sign(v_g - v)\cdot\tau_p, \; S(x,t)=4, \text{ for } |\tau| \le \tau_p \text{ and } S(x,t)=2;$$
$$\tau = sign(v_g - v)\cdot\tau_p, \text{ for } S(x,t)=4 \text{ and } \tau\cdot(v_g - v) \ge 0;$$
$$\tau = \tau_s + k_5(u_g - u - U_s), \; S(x,t)=5, \text{ for } \tau\cdot(v_g - v) < 0 \text{ and } S(x,t)=4;$$
$$\tau = \tau_s + k_5(u_g - u - U_s), \text{ for } S(x,t)=5 \text{ and } |\tau| < \tau_p;$$
$$\tau = sign(v_g - v)\cdot\tau_p, \; S(x,t)=4, \text{ for } |\tau| \ge \tau_p \text{ and } S(x,t)=5,$$

with initial conditions

$$u\,|_{t=0} = 0 \text{ and } v\,|_{t=0} = 0,$$

and also with stress-free boundary conditions, that is, with zero deformations

$$\frac{\partial u}{\partial x}\Big|_{x=0} = 0 \text{ and } \frac{\partial u}{\partial x}\Big|_{x=L} = 0.$$

Here:

$c = \sqrt{E/\rho}$ – wave propagation velocity in the pipeline;

E, ρ – modulus of elasticity and density of the pipeline material;

ε, v, u – deformation, velocity and movement of particles along the pipeline axis;

v_g, u_g – velocity and movement of soil particles along the pipeline axis;

D, F – diameter and cross-sectional area of the pipeline;

k_1 – coefficient of elastic interaction of the pipeline surface with the ground;

$k_2 < 0$ – the coefficient of interaction in the field of destruction;

k_3, k_5 – coefficients of interaction in the unloading area;

$k_4 = 0$ – the coefficient of interaction in the field of interaction according to the law of dry friction;

τ^* – absolute values of the limit of tangential stress, after which the destruction of the soil structure begins;

τ_p – the value of the tangential stress, after the completion of the destruction of the soil structure;

τ_s, U_s – the value of the lateral tangential stress and the difference between the displacements of the corresponding points of the soil and the pipeline at the moment of the *s*-th transition from one state to another $(\tau_0 = 0;\ U_0 = 0)$.

Experimental data [4, 5] showed that the values of k_1, k_2, k_3, k_5 and τ_p depend on static and dynamic pressure, as well as on the loading rate. The loading velocity should correspond to seismic waves [5], and the dynamic pressure [4] should be calculated through three components of displacement in a seismic wave, since most pipelines are located close to the earth's surface. For the convenience of analyzing the solutions obtained, we take the values k_1, k_2, k_3, k_5 and τ_p as constants.

Upon completion of the destruction, which is determined by the value of τ_p, the process takes place according to the dry friction model with elastic unloading. Transitions from one state to another state at each point along the x coordinate will occur repeatedly, depending on the wave processes in the pipeline and the ground.

It is necessary to pay attention to two circumstances: the wave propagation velocities in the ground and the pipeline differ several times, and the interaction of the pipeline with the ground is described by a piecewise linear model.

Let's break the pipeline of length L into segments of size Δx by m of parts $L = m\Delta x$. Using the t variable, we determine the $\Delta t = \Delta x / c$ time step, which is the limiting condition for the necessary stability of the Courant for an explicit finite-difference scheme. Let's introduce the notation: $q = \pi D / F\rho$.

We will take discrete values of deformation at the ends of the segments Δx, and the particle velocities in the middle of the segments Δx. In time, we will take discrete values of deformation in the middle of the step, and particle velocities at each step in time.

Let's imagine equations (1) by their finite-difference approximation of the first order of accuracy Δx and Δt.

$$\frac{v_{i+1/2}^{j+1} - v_{i+1/2}^{j}}{\Delta t} = c^2 \frac{\varepsilon_{i+1}^{j+1/2} - \varepsilon_{i}^{j+1/2}}{\Delta x} + q \frac{\tau_{i+1/2}^{j+1} + \tau_{i+1/2}^{j}}{2};$$
$$\frac{\varepsilon_{i+1}^{j+1/2} - \varepsilon_{i}^{j-1/2}}{\Delta t} = \frac{v_{i+1/2}^{j} - v_{i-1/2}^{j}}{\Delta x}, \qquad (2)$$

$$\tau_{i+1/2}^{j+1} = k_1\left(u_{g\,i+1/2}^{\;j+1} - u_{i+1/2}^{j} - \Delta t\; v_{i+1/2}^{j+1}\right), \text{ for } \left|\tau_{i+1/2}^{j+1}\right| \le \tau^* \text{ and } S_{i+1/2}^{j+1} = 1;$$
$$\tau_{i+1/2}^{j+1} = \tau_{i+1/2,s} + k_2\left(u_{g\,i+1/2}^{\;j+1} - u_{i+1/2}^{j} - \Delta t\; v_{i+1/2}^{j+1} - U_{i+1/2,s}\right), S_{i+1/2}^{j+1} = 2, \text{ for } \left|\tau_{i+1/2}^{j+1}\right| > \tau^* \text{ and } S_{i+1/2}^{j+1} = 1;$$
$$\tau_{i+1/2}^{j+1} = \tau_{i+1/2,s} + k_2\left(u_{g\,i+1/2}^{\;j+1} - u_{i+1/2}^{j} - \Delta t\; v_{i+1/2}^{j+1} - U_{i+1/2,s}\right), \text{ for } S_{i+1/2}^{j+1} = 2 \text{ and } \left|\tau_{i+1/2}^{j+1}\right| \ge \tau_p;$$
$$\tau_{i+1/2}^{j+1} = \tau_{i+1/2,s} + k_3\left(u_{g\,i+1/2}^{\;j+1} - u_{i+1/2}^{j} - \Delta t\; v_{i+1/2}^{j+1} - U_{i+1/2,s}\right), S_{i+1/2}^{j+1} = 3, \text{ for } \tau_{i+1/2}^{j+1} \cdot (v_{g\,i+1/2}^{j+1} - v_{i+1/2}^{j+1}) < 0 \text{ and } S_{i+1/2}^{j+1} = 2;$$
$$\tau_{i+1/2}^{j+1} = \tau_{i+1/2,s} + k_3\left(u_{g\,i+1/2}^{\;j+1} - u_{i+1/2}^{j} - \Delta t\; v_{i+1/2}^{j+1} - U_{i+1/2,s}\right), \text{ for } S_{i+1/2}^{j+1} = 3 \text{ and } \left|\tau_{i+1/2}^{j+1}\right| \le \left|\tau_{i+1/2,s}\right|;$$
$$\tau_{i+1/2}^{j+1} = \tau_{i+1/2,s} + k_2\left(u_{g\,i+1/2}^{\;j+1} - u_{i+1/2}^{j} - \Delta t\; v_{i+1/2}^{j+1} - U_{i+1/2,s}\right), S_{i+1/2}^{j+1} = 2, \text{ for } \left|\tau_{i+1/2}^{j+1}\right| > \tau_{i+1/2,s} \text{ and } S_{i+1/2}^{j+1} = 3;$$
$$\tau_{i+1/2}^{j+1} = sign(v_{g\,i+1/2}^{j+1} - v_{i+1/2}^{j+1}) \cdot \tau_p,\; S_{i+1/2}^{j+1} = 4, \text{ for } \left|\tau_{i+1/2}\right| \le \tau_p \text{ and } S_{i+1/2}^{j+1} = 2;$$
$$\tau_{i+1/2}^{j+1} = sign(v_{g\,i+1/2}^{j+1} - v_{i+1/2}^{j+1}) \cdot \tau_p, \text{ for } S_{i+1/2}^{j+1} = 4 \text{ and } \tau_{i+1/2}^{j+1} \cdot (v_{g\,i+1/2}^{j+1} - v_{i+1/2}^{j+1}) \ge 0;$$
$$\tau_{i+1/2}^{j+1} = \tau_{i+1/2,s} + k_5\left(u_{g\,i+1/2}^{\;j+1} - u_{i+1/2}^{j} - \Delta t\; v_{i+1/2}^{j+1} - U_{i+1/2,s}\right), S_{i+1/2}^{j+1} = 5, \text{ for } \tau_{i+1/2}^{j+1} \cdot (v_{g\,i+1/2}^{j+1} - v_{i+1/2}^{j+1}) < 0 \text{ and } S_{i+1/2}^{j+1} = 4;$$
$$\tau_{i+1/2}^{j+1} = \tau_{i+1/2,s} + k_5\left(u_{g\,i+1/2}^{\;j+1} - u_{i+1/2}^{j} - \Delta t\; v_{i+1/2}^{j+1} - U_{i+1/2,s}\right), \text{ for } S_{i+1/2}^{j+1} = 5 \text{ and } \left|\tau_{i+1/2}^{j+1}\right| < \tau_p;$$
$$\tau_{i+1/2}^{j+1} = sign(v_{g\,i+1/2}^{j+1} - v_{i+1/2}^{j+1}) \cdot \tau_p,\; S_{i+1/2}^{j+1} = 4, \text{ for } \left|\tau_{i+1/2}^{j+1}\right| \ge \tau_p \text{ and } S_{i+1/2}^{j+1} = 5;$$

$$u_{i+1/2}^{j+1} = u_{i+1/2}^{j} + \Delta t\left(v_{i+1/2}^{j+1} + v_{i+1/2}^{j}\right)/2;$$
$$u_{g\,i+1/2}^{j+1} = u_{g\,i+1/2}^{j} + \Delta t\left(v_{g\,i+1/2}^{j+1} + v_{g\,i+1/2}^{j}\right)/2,$$

where the lower index corresponds to the coordinate, and the upper one corresponds to the time. A sufficient condition for the stability of the difference scheme (2) is the following condition: $q \cdot k_1 \cdot (\Delta t)^2 << 1$

From equations (2) we define sequentially: $\varepsilon_{i+1}^{j+1/2}, v_{i+1/2}^{j+1}, u_{i+1/2}^{j+1}, u_{g\,i+1/2}^{j+1}$. At each time step, we check the values τ, $\tau \cdot (v_g - v)$ and $(u_g - u)$ at all points. At those points where the transition to the next state occurs, we perform iterative refinement of the solution by the Newton-Raphson method [9]

$$\Delta v^{(k)} = -\left(v_{i+1/2}^{j+1}\right)^{(k)} + \frac{2c\left(\varepsilon_{i+1}^{j+1/2} - \varepsilon_{i}^{j+1/2}\right) + 2v_{i+1/2}^{j} + 2q\Delta t\tau_{i+1/2,s} + k_{\alpha}q\Delta t\left(u_{g\,i+1/2}^{j+1} + u_{g\,i+1/2}^{j} - 2u_{i+1/2}^{j} - 2U_{i+1/2,s}\right)}{2 + k_{\alpha}q(\Delta t)^2},$$

$$\left(v_{i+1/2}^{j+1}\right)^{(k+1)} = \left(v_{i+1/2}^{j+1}\right)^{(k)} + \Delta v^{(k)},$$

where k - iteration number. The iterative process continues until the required accuracy of the v calculation is achieved. We will save information about the transition at each point of discredit, where the transition from one state to another occurs, the values of $\tau_s = \tau, U_s = u_g - u$.

In the subsequent time steps, calculations are performed in accordance with the state of the interaction process at each point.

RESULTS AND DISCUSSION

Calculations were performed with the following initial data: $L = 1000\, m$; $D = 0.61\, m$; $F = 0.019\, m^2$; $c_g = 500\, m/s$; $c = 5000\, m/s$; $k_1 = 10^7\, N/m^3$; $k_2 = -5\cdot 10^6\, N/m^3$; $k_3 = k_5 = 10^7\, N/m^3$; $\tau_p = 10\, kPa$; $\tau^* = 14\, kPa$; $\Delta t = 0.0001\, s$.

Let's calculate the action of the harmonic velocity wave in the form of $v_g = v_{gm}\cos[\pi(t - x/c_g)/t_0]H(t - x/c_g)$, amplitude $v_{gm} = 0.19\, m/s$, where $H(t)$ – Heaviside function, $t_0 = 0.165\, s$ corresponds to the dominant half-period of the earthquake seismogram.

Fig. 2 shows normalized graphs of $\varepsilon_{gn} = \varepsilon_g / \varepsilon_{gm}$ soil deformation (here $\varepsilon_{gm} = 0.00038$) and the pipeline $\varepsilon_n = \varepsilon / \varepsilon_{gm}$ at various points in time. The same values for the model of an ideal elastic-plastic body are presented in the form of ε'_n. As can be seen from these graphs, the deformation of the pipeline, taking into account the destruction of the soil, differs very little from the deformation with an ideally elastic-plastic interaction. This is due to the relatively large value of $t_0 = 0.165\, s$, the destruction process occurs in a short time, and the hysteresis area is determined mainly due to the dry friction area. If the period of the wave propagating in the ground is much smaller (high-frequency wave), then the effect of the process of destruction of the soil structure in the vicinity of the pipeline on the values of deformations will be significant.

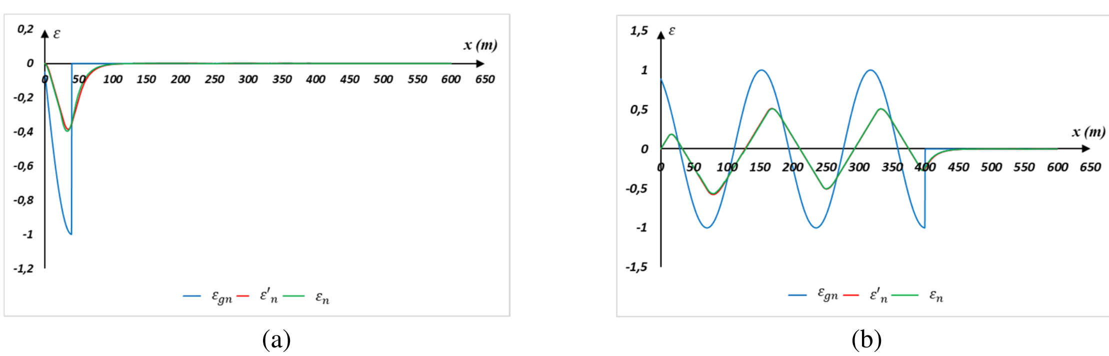

FIGURE 2. Normalized strains in soil of $\varepsilon_{gn} = \varepsilon_g / \varepsilon_{gm}$ and the pipeline $\varepsilon_n = \varepsilon / \varepsilon_{gm}$ at points in time: *t=0.08 s* (a) and *t=0.8 s* (b).

Fig. 3 shows normalized graphs of the velocities of the $v_{gn} = v_g / v_{gm}$ soil particles and the $v_n = v / v_{gm}$ pipeline at various points in time. The same values for the model of an ideal elastic-plastic body are presented in the form of v'_n. From the graphs in Fig. 3, one can see the effect of the difference in the velocities of wave propagation in the ground and pipeline. Because of this, ahead of the wave front of the velocities of the soil particles, there is a wave in the pipeline with rapid attenuation due to the transfer of wave energy through elastic bonds. It can also be noted here that the particle velocities are very close according to different interaction models, as are deformations.

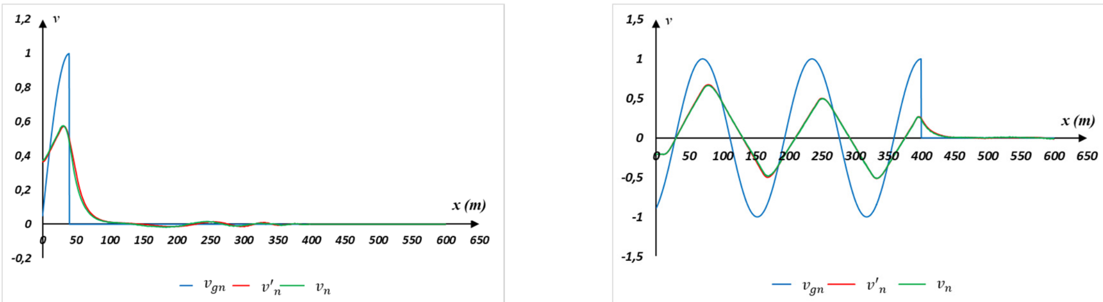

(a) (b)

FIGURE 3. Dimensionless velocities of soil $v_{gn} = v_g / v_{gm}$ and the pipeline $v_n = v / v_{gm}$ particles at points in time: *t=0.08 s* (a) and *t=0.8 s* (b).

Figure 4 shows graphs of the movement of the u_g soil and the u pipeline at various points in time. The same values for the model of an ideal elastic-plastic body are presented in the form of u'. This is as a result of the integration of particle velocities, the asymmetry of velocities and displacements relative to the Ox axis is due to the presence of a wave front, i.e., the non-stationarity of the process, and the nonlinearity of the interaction law.

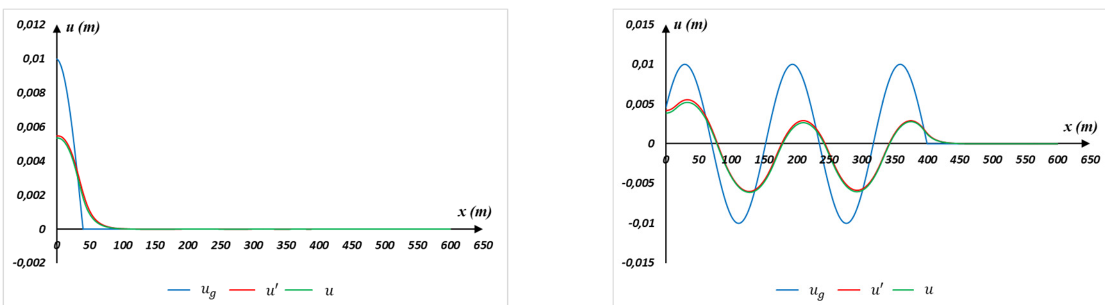

(a) (b)

FIGURE 4. Displacements (in meters) of the ground and the pipeline at points in time: *t=0.08 s* (a) and *t=0.8 s* (b).

Fig. 5 shows normalized graphs of the lateral tangential stress $\tau_n = \tau / \tau_p$ at different points in time. The same values for the model of an ideal elastic-plastic body are represented in the form τ'_n. Here you can see the difference in tangential stresses when using different interaction models.

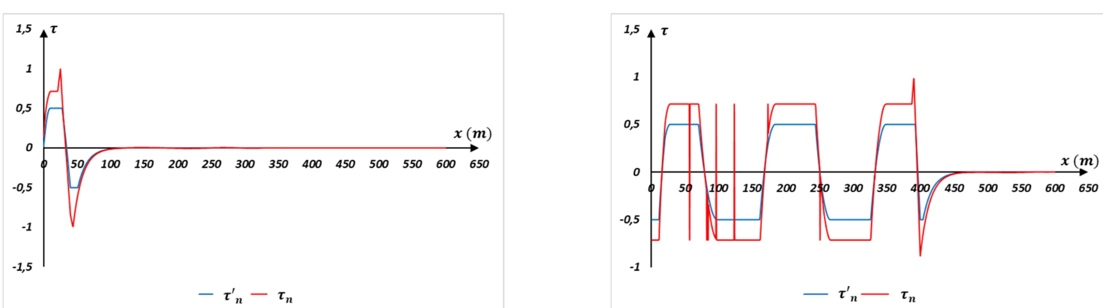

(a) (b)

FIGURE 5. Normalized lateral tangential stress $\tau_n = \tau / \tau_p$ at time points: *t=0.08 s* (a) and *t=0.8 s* (b).

In the case of the model of ideal elastic-plastic interaction, transitions from the dry friction state to the unloading state and the reverse transition to the dry friction state can occur in a short time (0.0005 s). The transition through the destruction of the soil structure is observed only near the front of the wave propagating in the soil.

Now we assume that a given velocity wave propagates through the ground in the form of a pulse $v_g = v_{gm}[H(t - x/c_g) - H(t - t_0/2 - x/c_g)] - v_{gm}[H(t - t_0/2 - x/c_g) - H(t - t_0 - x/c_g)]$.

Fig. 6 shows normalized graphs of the velocities of the $v_{gn} = v_g / v_{gm}$ soil particles and the $v_n = v / v_{gm}$ pipeline at various points in time. The same values for the elastic interaction model are presented in the form of v'_n. The graphs of Fig. 6 shows the effect of nonlinearity of the interaction, the shape of the momentum is very different from the shape of the momentum of the elastic interaction. Due to the appearance of areas of destruction of the soil structure and dry friction, the wave caused by the negative part of the momentum of the velocity of the soil particles catches up with the front part of the wave in the pipeline. Therefore, over time, a wave with a positive particle velocity disappears in the front part, which does not exist in the case of elastic interaction. The same patterns can be observed in Fig. 7 and Fig. 8 for deformation and displacement.

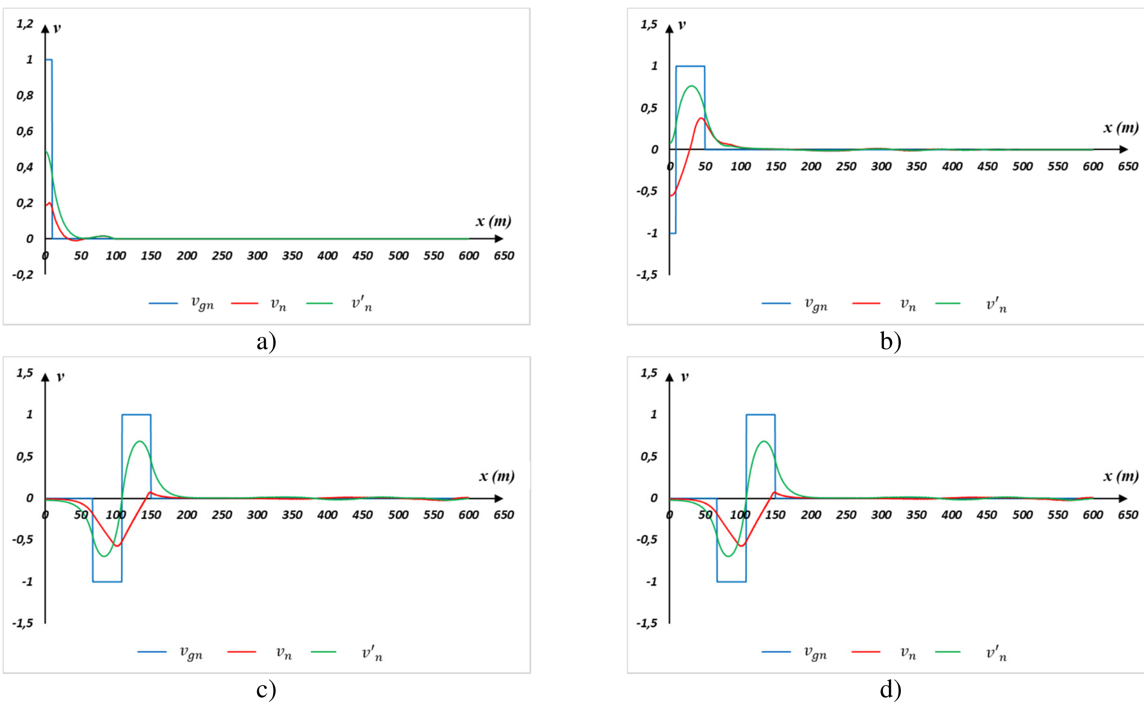

FIGURE 6. Dimensionless velocities of soil $v_{gn} = v_g / v_{gm}$ and the pipeline $v_n = v / v_{gm}$ particles at points in time: *t=0.02 s* (a), *t=0.1 s* (b), *t=0.3 s* (c) and *t=0.6 s* (d).

Fig. 7 shows normalized graphs of $\varepsilon_{gn} = \varepsilon_g / \varepsilon_{gm}$ soil deformation and the pipeline $\varepsilon_n = \varepsilon / \varepsilon_{gm}$ at various points in time. The same values for the elastic interaction model are presented in the form of ε'_n.

Figure 8 shows graphs of the movement of the u_g soil and the u pipeline at various points in time. The same values for the elastic interaction model are presented in the form of u'.

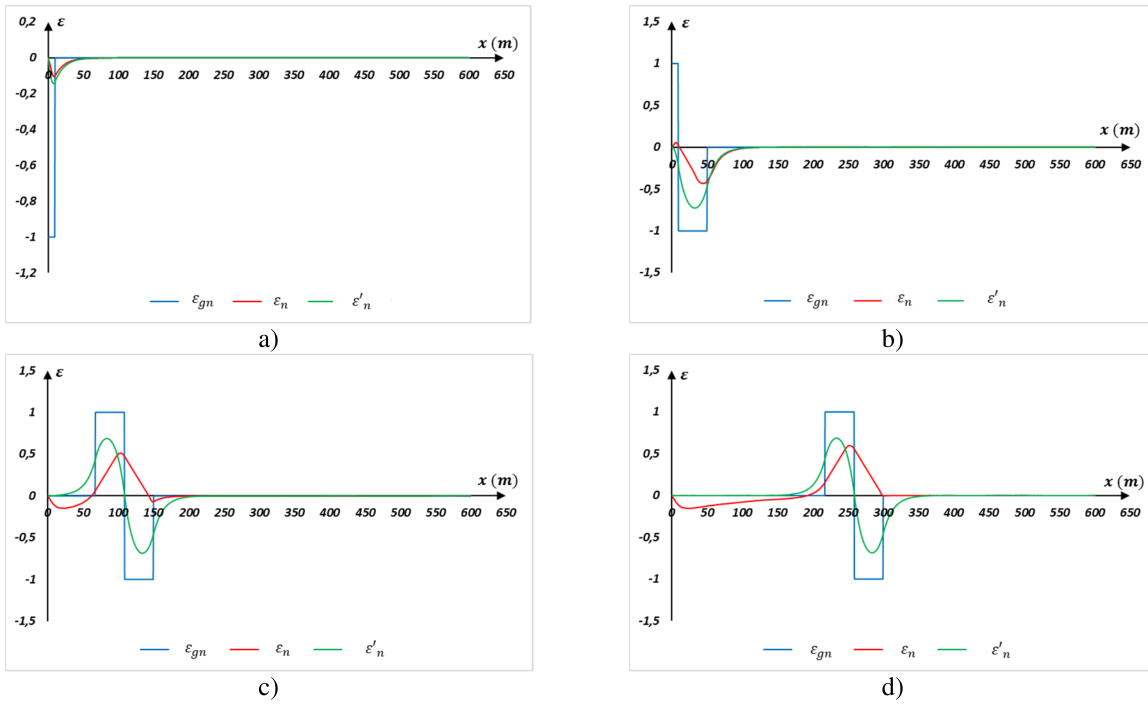

FIGURE 7. Normalized strains in soil of $\varepsilon_{gn} = \varepsilon_g / \varepsilon_{gm}$ and the pipeline $\varepsilon_n = \varepsilon / \varepsilon_{gm}$ at points in time: *t=0.02 s* (a), *t=0.1 s* (b), *t=0.3 s* (c) and *t=0.6 s* (d).

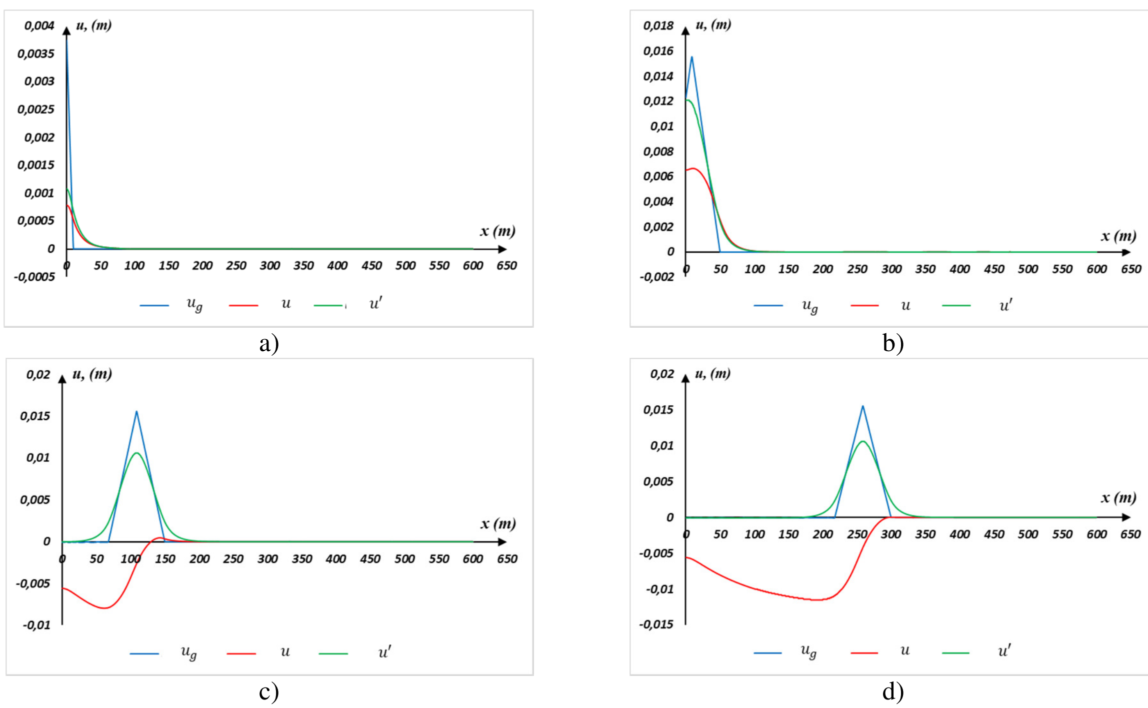

FIGURE 8. Displacements (in meters) of the ground and the pipeline at points in time: *t=0.02 s* (a), *t=0.1 s* (b), *t=0.3 s* (c) and *t=0.6 s* (d)

Fig. 9 shows normalized graphs of the lateral tangential stress $\tau_n = \tau / \tau_p$ at different points in time. The same values for the elastic interaction model are presented in the form of τ'_n.

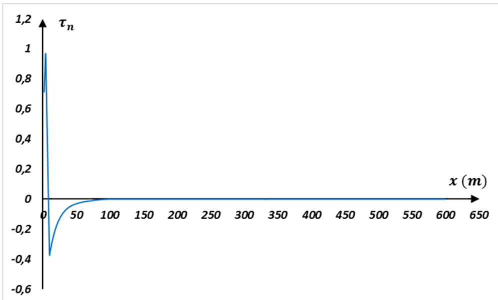

a)

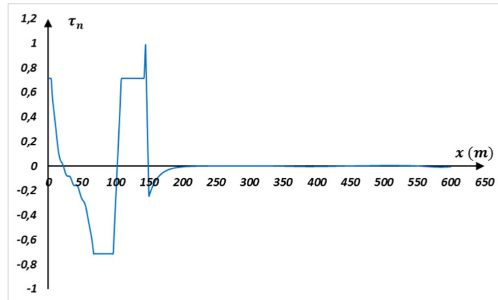

c)

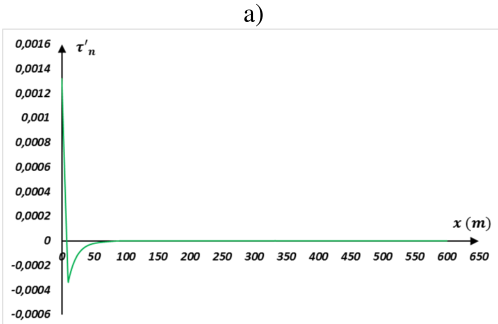

b)

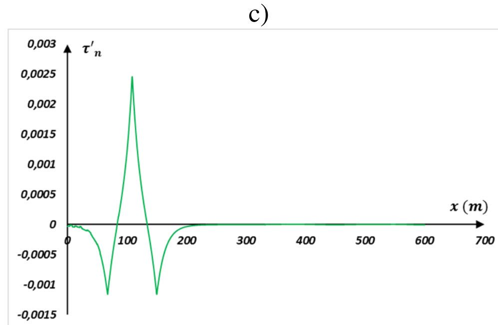

d)

FIGURE 9. Normalized lateral tangential stress $\tau_n = \tau / \tau_p$ at time points: *t=0.02 s* (a, b) and *t=0.3 s* (c, d)

In the graphs, Fig. 9a and Fig. 9b show changes in the shear stress on the lateral surface of the pipeline along its length at time *t=0.02 s* for nonlinear and linear interactions, respectively. And the graphs in Fig. 9c and Fig. 9d show in the same way the changes in the tangential stress on the lateral surface of the pipeline along its length at the time *t=0.3 s*.

CONCLUSION

The method of finite differences according to an explicit scheme solves the non-stationary problem of the effect of a plane longitudinal wave propagating in the ground on an underground pipeline of finite length when it interacts with the ground according to the model with the destruction of the soil structure. The obtained results are compared with the corresponding results in the cases of models of elastic interaction and an ideal elastic-plastic body. The process of wave formation and propagation in the pipeline is shown. Residual phenomena after the passage of the wave depend on the waveform. For a sinusoidal wave in the ground, the output to the stationary mode of wave propagation in the pipeline is shown, which differs in shape from the results of elastic interaction.

A comparison of the results of the effects of a wave propagating in the ground by models taking into account the failure of the ground structure and an ideal elastic-plastic body showed that the interaction model in the form of an "ideal elastic-plastic body" can be used in calculations for seismic waves from earthquakes. The influence of the nonlinearity of the interaction is reflected in the shape of the pulse, which is very different from the shape of the pulse of the elastic interaction. Due to the appearance of areas of destruction of the soil structure and dry friction, the wave caused by the negative part of the momentum of the velocity of the soil particles catches up with the front part of the wave in the pipeline. Therefore, over time, a wave with a positive particle velocity disappears in the front part, in the case of elastic interaction, such a picture is not observed.

REFERENCES

1. T. Rashidov, *Dynamic theory of seismic resistance of complex systems of underground structures,* (in russian) (1973). URL: https://ru.b-ok.as/book/2975567/59d466
2. L. Muravyeva and N. Vatin, *Appl. Mech. Mater.,* (2014). https://doi.org/10.4028/www.scientific.net/AMM.635-637.468
3. D. V. Georgievskii and M. S. Israilov, Mech. Solids **50**, (2015). https://doi.org/10.3103/S0025654415040135
4. K. Sultanov and N. Vatin, Appl. Sci. **11**, 1797 (2021). https://doi.org/10.3390/app11041797
5. K. R. Massarsh, *Urban Renovation and Geotechnical Construction No 9*, (in russian) (2005). URL: https://dwg.ru/dnl/8184
6. E. Kosimov, I. Mirzaev and D. Bekmirzaev, *IOP Conf. Ser. Mater. Sci. Eng.* (2021). https://doi.org/10.1088/1757-899X/1030/1/012082
7. I. Mirzaev and V. S. Nikiforovskii, *Soviet Mining Science* **9**, (1973). https://doi.org/10.1007/BF02506181
8. V. Corrado, B. D'Acunto, N. Fontana and M. Giugni, Math. Probl. Eng. **2012**, (2012). https://doi.org/10.1155/2012/824578
9. K. A. Chopra, *Numerical Evaluation of Dynamic Response* (2012). URL: http://faculty.tafreshu.ac.ir/file/download/course/1587566331-dynamic.of.structures.chopra.4th-www.ucivil.ir.pdf
10. D. A. Bekmirzaev and I. Mirzaev, Soil Mech. Found. Eng. **57**, 491 (2021). https://doi.org/10.1007/s11204-021-09697-0
11. I. Mirzaev and J. F. Shomurodov, J. Phys. Conf. Ser. **1902**, (2021). https://doi.org/10.1088/1742-6596/1902/1/012017
12. B. Khusanov and B. Rikhsieva, *E3S Web Conf.* (2019). https://doi.org/10.1051/e3sconf/20199704040
13. M. Sh. Israilov, 15th World Conf. Earthq. Eng. (2012). URL: https://www.iitk.ac.in/nicee/wcee/article/WCEE2012_2125.pdf
14. S. Okamoto, *Introduction to Earthquake Engineering* (1984).
15. M. J. O'Rourke and X. Liu, *Multidisciplinary Center for Earthquake Engineering Research* (1999).
16. S. Toprak, F. Taskin and A. Cem Koc, Bull. Eng. Geol. Environ. **68**, (2009). https://doi.org/10.1007/s10064-009-0230-1
17. T. D. O'Rourke, S. S. Jeon, S. Toprak, M. Cubrinovski, M. Hughes, S. Van Ballegooy and D. Bouziou, Earthq. Spectra **30**, (2014). https://doi.org/10.1193/030413EQS062M
18. M. Erdik, T. Rashidov, E. Safak and A. Turdukulov, Soil Dyn. Earthq. Eng. **25**, (2005). https://doi.org/10.1016/j.soildyn.2004.11.002
19. L. Muravyeva and N. Vatin, *Appl. Mech. Mater.* (2014). https://doi.org/10.4028/www.scientific.net/AMM.633-634.958
20. L. V. Nikitin, Statics and dynamics of rigid bodies with external dry friction, (in Russian) (1998). URL: https://www.twirpx.com/file/1003867
21. R. I. Mogilevsky, T. O. Ormonbekov and L. V. Nikitin, J. Mech. Behav. Mater. **5**, 85 (1993). https://doi.org/10.1515/JMBM.1993.5.1.85